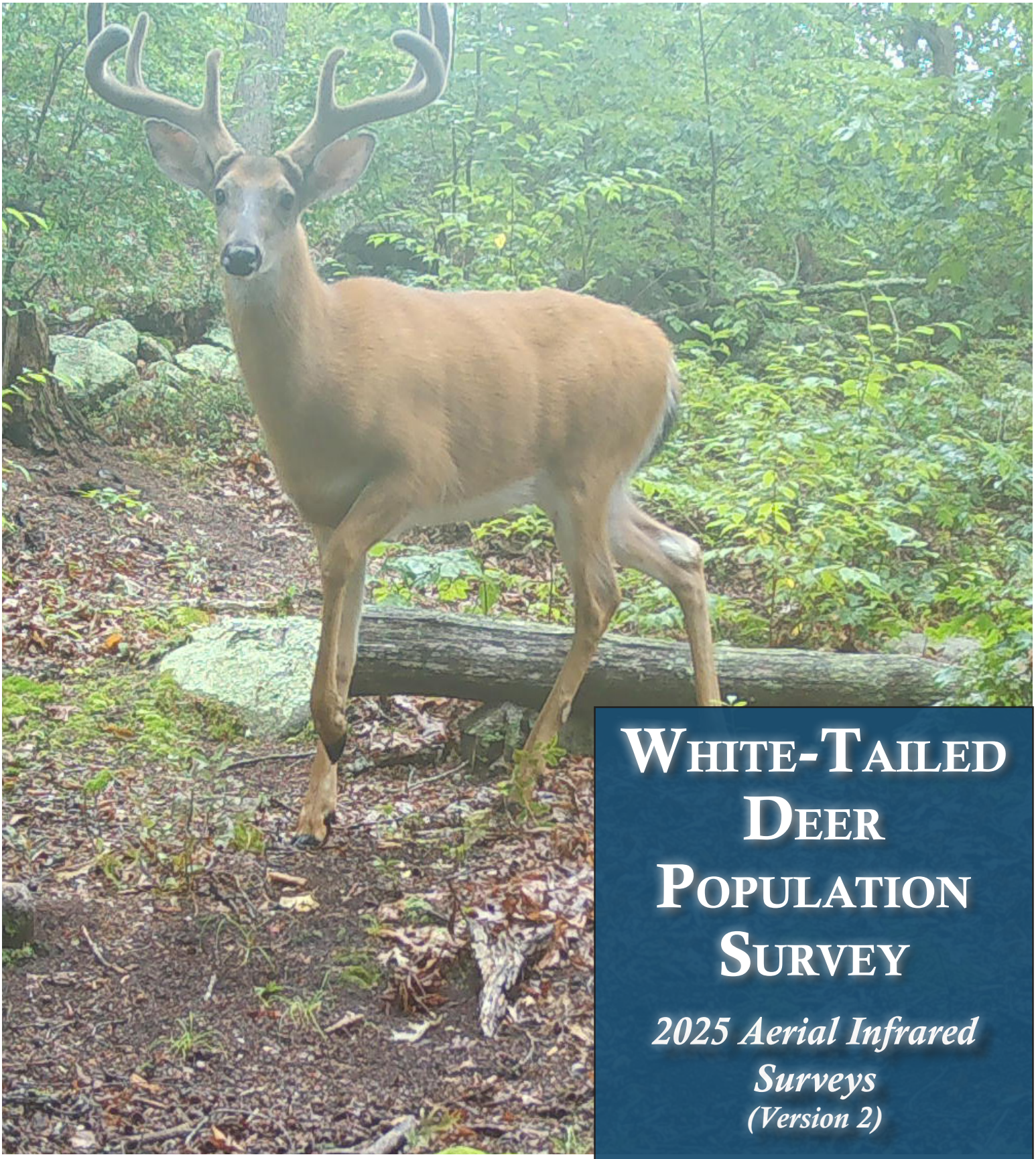

White-Tailed Deer Population Survey

2025 Aerial Infrared Surveys

(Version 2)

Report Prepared By:

Amy Mayer, Kathleen Carroll, Jason Parent & Brian Gerber

University of Rhode Island

Department of Natural Resources Science

Introduction

Accurate estimations of the abundance and distribution of the white-tailed deer population in Rhode Island are critical for appropriate management. Harvest records are typically the primary source of information on white-tailed deer populations; however, aerial surveys have been used to supplement and validate this information. The last aerial survey was conducted in 2017 via fixed-wing aircraft with a FLIR (forward-looking infrared) camera. This survey covered a small portion of the state – a total of 13 1-mile^2 blocks (excluding Block Island) - and the contractors reported a total of 584 deer counted within these blocks. In 2022 we provided further analysis on the 2017 FLIR data set and estimated the deer abundance to be 50,532 (95% C.I. 46,801 – 54,560). While the land cover represented in the survey blocks was proportionate to the total land cover in the state, the total area surveyed covered only approximately 1% of the state's land area and was not sufficient to neither capture spatial variation in deer densities nor produce an accurate abundance estimate.

In February 2025, DEM initiated an aerial infrared survey to cover a larger area of the state with 78 1-mile spaced transects, as well as fully capture the entire area from three focus areas - Dutch Island, Colt State Park, and Patience Island - with 200-ft spaced transects (**Figure 1**). The goal of these surveys was to collect sufficient data to accurately measure deer abundance, and to provide additional data to supplement harvest and camera trap records.

Here we present the results of the survey along with a detailed explanation of the limitations of the data collected and results. We also offer recommendations for future aerial surveys to improve the results, as well as alternative/additional data collection methods that may be incorporated into future analyses. Based on surveys done on other species, both across New England and other geographies, we expected that deer detection and abundance estimations would be affected by temperature (with warmer temperatures making estimation more challenging), sampling height (with lower flying heights more conducive to higher accuracy), and image pixel depth/camera quality (with higher quality images and deeper pixel depth resulting in more accurate deer counts).

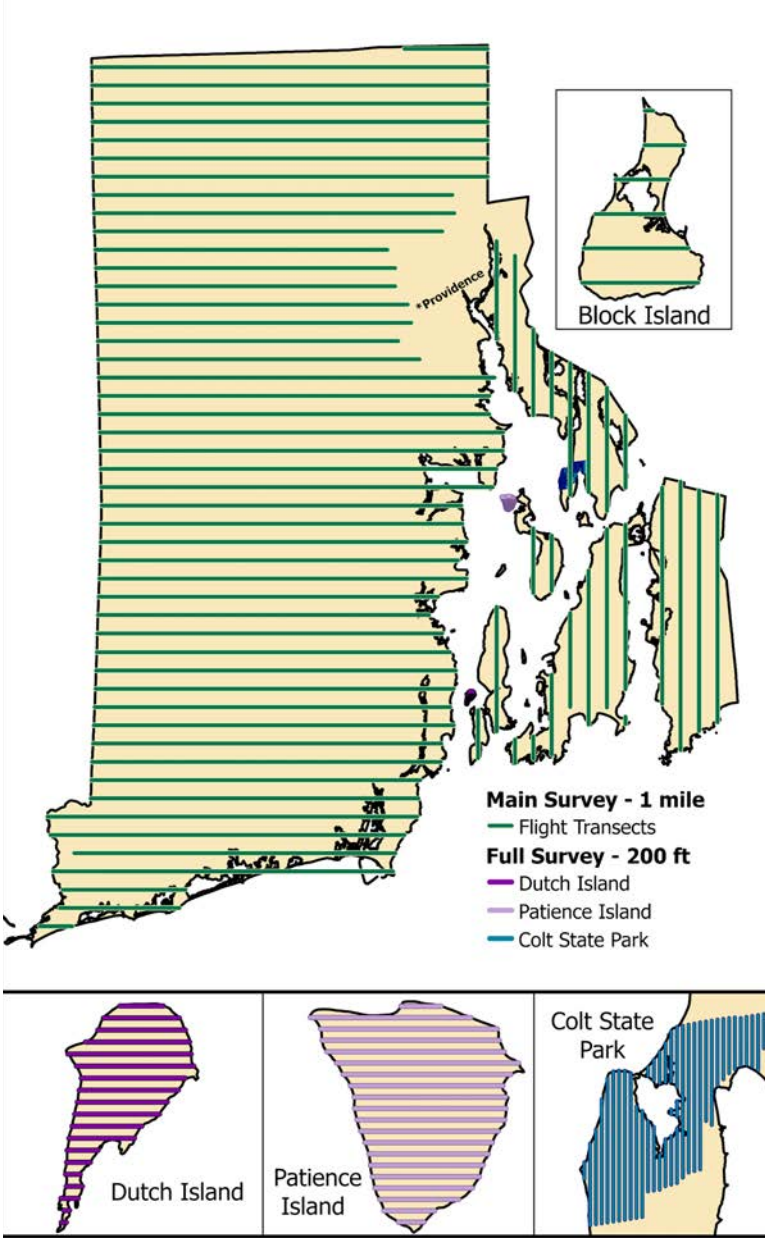

Figure 1. *The sampling study design for Rhode Island. Transects were flown with 1 mile spacing between routes. Three focal areas - Dutch Island, Patience Island, and Colt State Park - had full surveys, all flown with 200 ft between routes.*

Methods

Data Collection

Jeff Codman of Newport Helicopter Tours conducted survey flights in the winter of 2025. A Teledyne FLIR Vue Pro-R Radiometric Infrared Camera for sUAS, programmed to collect one still image every second, was affixed to the helicopter and oriented vertically towards the ground. The pilot was instructed to fly along the pre-set transects at an altitude of approximately 200 m and a speed of approximately 50 knots; however, altitude and speed were adjusted as necessary to maintain safe flying conditions. He conducted survey flights at night in February and March, typically between 6:00 p.m. and 1:00 a.m. We selected February and early March as the target survey months because weather conditions are typically favorable during these months, while avoiding overlap with the peak deer hunting season.

Imagery Processing

We georeferenced all images collected during the flight to the best of our ability, given the provided metadata. We extracted the coordinates and flight altitude above the ground (AGL) from each image. In the metadata, roll, pitch, and yaw were all recorded as 0; however, the infrared camera was not mounted on a gimbal but rather attached directly to the helicopter. Therefore, any deviations from horizontal to the ground experienced by the helicopter were not recorded, which caused errors in the georeferenced positions of the images. Due to these limitations, we chose to process imagery outside of a GIS and use georeferenced image centroids to approximate survey image locations.

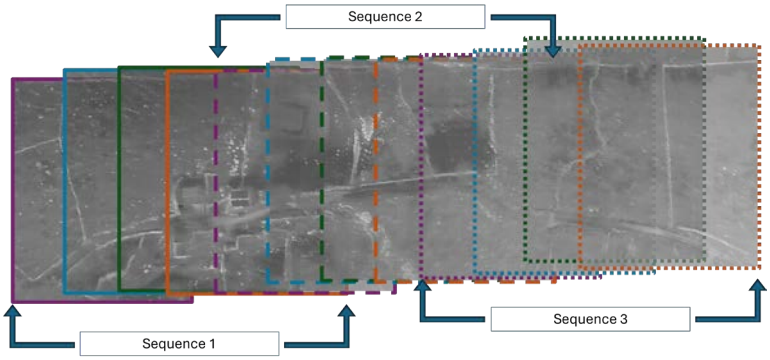

Figure 2. *Individual images were sorted into image sequences to account for overlap and avoid double-counting in the processing workflow.*

Table 1. *Each sequence was assigned an observer estimate and confidence value. These values were used to convert to a minimum and maximum estimate for each sequence. All minimum values were ≥ 0.*

Confidence value	Observer Estimate = 0	Observer Estimate > 0
1 – Very Confident	0	Estimate
2 – Confident	0 – 2	Estimate +/- 1 (range of 3)
3 – Neutral	0 – 4	Estimate +/- 2 (range of 5)
4 – Uncertain	0 – 8	Estimate +/- 4 (range of 9)
5 – Very Uncertain	0 - 12	Estimate +/- 6 (range of 13)

All images were sorted into image sequences based on their AGL which corresponded to the actual space the images covered on the ground. (**Figure 2)**. Each image overlapped subsequent images, and sorting images into sequences or groups allowed us to avoid double-counting any deer detected in the images by attributing an estimate to a sequence rather than to individual images. To quantify uncertainty in our count estimates, we developed a confidence value system that we later converted to a minimum and maximum value range (**Table 1**). For example, an estimate of 3 deer with a confidence level of 1 indicates that we had high certainty that our estimate is correct and that the image sequence indeed contains 3 deer. The associated range would then be 3 to 3. Alternatively, an estimate of 3 with a confidence value of 4 indicates that while our estimate was 3 deer in the image sequence, we had low certainty in that estimation. Thus, the associated range for that image sequence would be 0 to 8.

We resolved the overlap in all images by converting individual images to sequences; however, overlap between adjacent sequences remained. To avoid overestimating the population, we removed every-other sequence while retaining any non-adjacent estimates >0 (**Figure 3**). This ensured we were not double counting the same individuals along the transect, but also not double counting estimates of zero, as in many sequences, the uncertainty of our zeros results in a range that includes values >0.

Methods

Image Processing (cont'd)

Figure 3. *Example of final sequence footprints on the landscape after accounting for overlap between adjacent images and adjacent sequence groups.*

We set the average image sequence footprint area (250 m^2) as our survey unit size and calculated the relative amount of several land cover classes (forest, commercial/industrial development, residential development, open development [parks/golf courses, etc.], shrubland, and wetland) within each survey unit. We used the observed estimate and minimum/maximum estimates to fit negative binomial models. We evaluated combinations of land cover covariates that best explain the spatial variation of the estimated count data. Using the best-fit model, we then predicted the overall relative abundance, as well as the minimum and maximum abundance, taking into account the uncertainty in the observations. Thus, we generated three final models, one for the estimate, one for the lower uncertainty bound, and one for the upper uncertainty bound.

Focal Areas Processing Adjustments

Within the three focal areas (Dutch Island, Patience Island, and Colt State Park), there was nearly 100% spatial coverage with the infrared imagery. We followed the same processing procedure as above, where images were grouped into sequences to account for overlap along the transect; however, due to the tightly spaced transects, there was also overlap between the transects. After assigning estimates and ranges to each sequence, we used ArcPro to plot estimates on the map and visually removed any overlapping sequences. This prevented double-counting the same group of deer across transects and prevented double-counting estimates of zero that also had high uncertainty. The remaining sequences represented a full coverage snapshot of each focal area, allowing us to simply sum the estimates and the minimum and maximum range to produce population estimates with a measure of uncertainty.

Survey Results

The main survey, conducted with 1-mile spaced transects, was completed over 7 flights from March 3, 2025, to March 27, 2025 (**Figure 4; Table 2**). The imagery captured in these surveys covered a total of 211.2 km^2, or approximately 7.9% of the land area of Rhode Island. After processing all images and accounting for overlap between the images, there were 5,899 sequences along 77 transects that were used in the abundance analyses (**Table 3**). Observer certainty in the observed estimates varied due to flight altitudes (average 274 m AGL; 157 – 596 m AGL), weather/temperature conditions, and landscape characteristics.

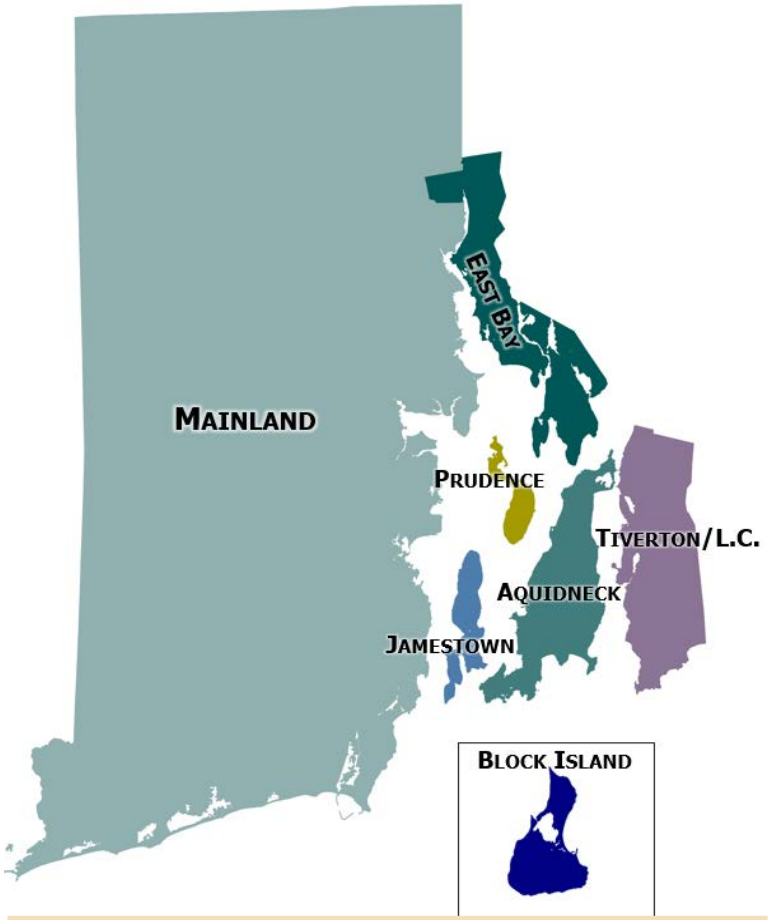

Figure 4. *Surveys were grouped into areas to simplify flight logisitics. The map above shows how Rhode Island was grouped into individual survey areas.*

Table 2. *Survey dates, locations, flight times, and survey weather conditions.*

Survey Date	Surveyed Area	Flight Times	Average Flight (°F)	Highest Daytime Temp. (°F)
2/19/2025	Patience, Colt	18:15 – 21:37	26.4	31
3/3/2025	Dutch, Block Island, Prudence, Jamestown, Aquidneck	18:06 – 20:51	30.25	34
3/10/2025	Mainland Transects 1-11	18:18 – 23:30	46.8	63
3/11/2025	Mainland Transects 12-17; 27-31	18:28 – 22:53	45.9	61
3/12/2025	Mainland Transects 18-20; 32-37	20:33 – 00:14	38	52
3/18/2025	Easy Bay (all), Mainland Transects 21-26; 38-39	20:33 – 01:44	39	63
3/23/2025	Mainland Transects 40-45	19:31 – 21:47	38.3	46
3/27/2025	Mainland Transects 46-49, Tiverton (all), Dutch post-cull	18:41 – 22:05	42.5	49

Survey Results

Table 3. *Total number of transects surveyed, and final count of image sequences used in the analysis.*

Survey Area	# Transects	# Sequences	# Zero Sequences	# > 0 Sequences
Mainland	48	4,911	4,325	586
Aquidneck	7	281	245	36
Block Island	6	87	79	8
East Bay	8	219	196	23
Jamestown	2	76	71	5
Tiverton	4	285	236	46
Prudence	2	40	32	8
Patience Island	11	62	52	10
Dutch Island Pre-Cull	12	30	21	9
Dutch Island Post-Cull	10	25	16	9
Colt State Park	27	145	123	22

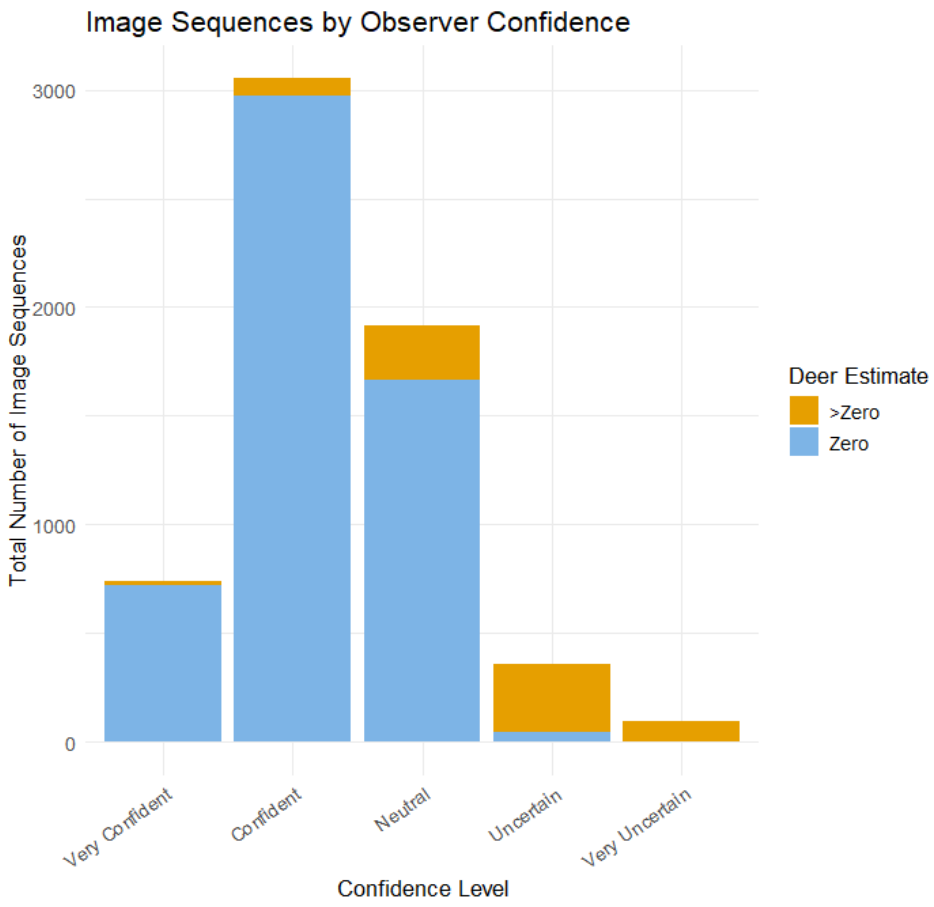

Figure 5. *Observer confidence in initial image sequence estimates. Observer confidence was influenced by landscape characteristics, flight attributes, and weather conditions.*

Only 12% (712) of the sequences included in the analyses had an initial observed count of >0 deer, while 88% (5,187) of sequences had an initial observed estimate of zero. The majority of sequences with initial zero estimates were considered confident, while the majority of estimates with initial estimates >0 were mostly uncertain (**Figure 5**).

Confidence values were converted to minimum and maximum estimates for each sequence. The minimum value was constrained to positive values; therefore, maximum values were inflated as the initial observer estimates were generally low. However, these inflated values highlight the uncertainty in the overall estimates (**Figure 6**).

Survey Results

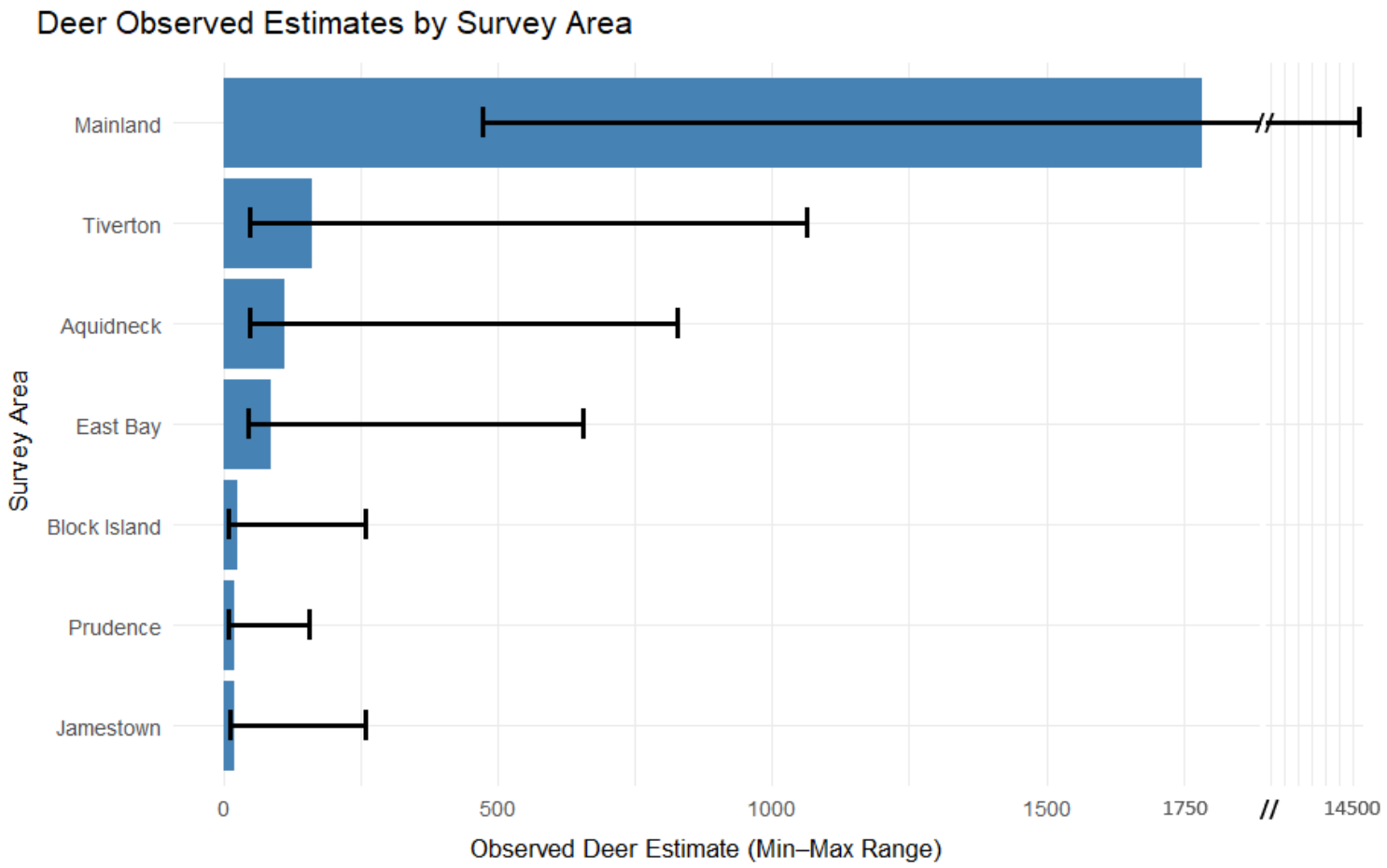

***Figure 6**. The observed estimate for each area of the 1-mile spaced transect surveys. Error bars indicate the minimum and maximum observed estimates for each survey area given observer confidence in the estimate.*

Focal Area Results

The focal area surveys were conducted over 3 nights, and Dutch Island was surveyed twice – before and after a planned deer cull (**Table 2**). Similar to the 1-mile spaced transect survey, our estimates were associated with a wide minimum-to-maximum estimate range indicating low confidence in the observed values (**Figure 7**). However, the comparison of observed values on Dutch Island pre- and post-cull were aligned with the known number of deer removed from the island (**Table 4**). The higher uncertainty in the estimate for the second Dutch Island survey highlights the importance of proper timing and weather conditions, as the second survey took place three weeks after the first, and when the average temperature had increased by >10°F.

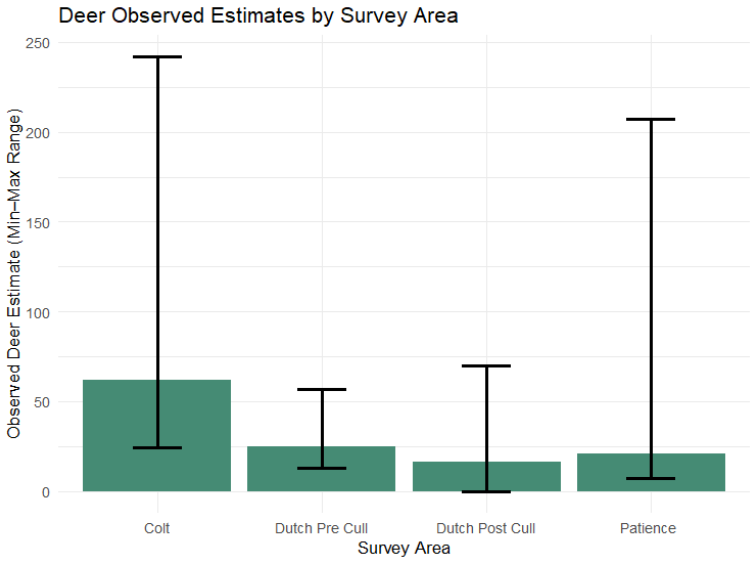

***Figure 7.** The observed estimate for each area of the areas. Error bars indicate the minimum and maximum observed estimates for each survey area given observer confidence in the estimate.*

Survey Results

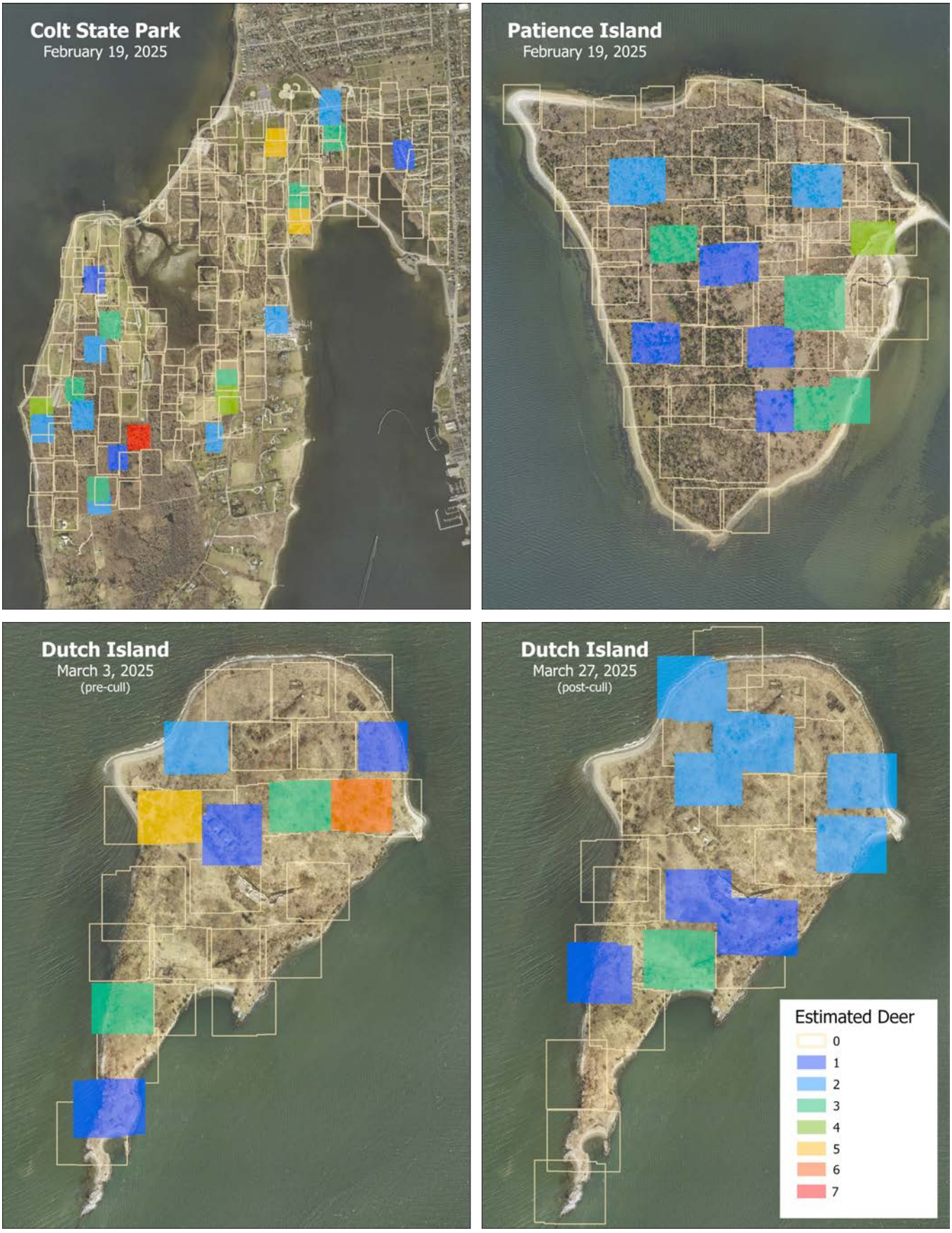

Figure 8. *Results from each of the three focal areas. Overlap between adjacent sequences and transects was resolved visually, so that no deer were double-counted. Dutch Island was surveyed pre- and post- deer cull.*

Survey Results

Focal Area	Abundance Estimate (min - max)	Estimated Density (min - max)	
		Deer/km²	*Deer/mile²*
Colt State Park	62 (24 - 242)	27 (10 - 105)	70 (27 - 272)
Patience Island	21 (7 - 207)	22 (7 - 215)	56 (19 - 556)
Dutch Island (pre-cull)	25 (13 - 57)	60 (31 - 137)	155 (81 - 354)
Dutch Island (post-cull)	16 (0 - 70)	36 (0 - 159)	94 (0 - 411)

Table 4. *Abundance and density estimates for each of the three focal areas. Abundance is the sum of counts of each included image sequence. Minumum and maximum values reflect uncertainty in the abundance estimate, where a wider range means more uncertainty in the abundance estimate.*

Modeling and Prediction Results

The best-fit negative binomial model included the forest (all types), agriculture, and residential development landscape covariates. All three had significant positive effects on deer abundance in the model, but the amount of forest in the survey unit had the strongest effect on abundance (**Table 5**). This best-fit model was run using three datasets/scenarios: the original observed count estimates, the minimum estimated count given uncertainty, and the maximum estimated count given uncertainty. These three models were then used to predict deer abundance across the state and create maps under each of the three scenarios. This allowed us to quantify and visualize both the estimated spatial abundance of the deer population and the uncertainty in this abundance estimate. The average estimated abundance statewide was 15,944 deer (**Table 6, Figure 9**). We did not predict to cells with very high amounts of development (>70%), or the highly urban areas of Providence as these areas were not captured in the survey flights.

Given the high uncertainty in the estimates highlighted by the discrepancy between the minimum and maximum deer estimates, we caution relying on these estimates alone for management purposes. However, the mean estimates generated during this survey are marginally aligned with previous analyses including the population reconstruction from Bellier et al. (2024), and the abundance estimates generated from previous winter season trail camera surveys (**Table 7**).

Covariate	Estimate	Std. Error	z-value	p-value	Interpretation
(Intercept)	-1.980	0.198	-9.974	< 2e-16	Baseline log count when all predictors = 0
Agriculture	1.719	0.379	4.536	5.74e-06	*Positive effect*: more agriculture → higher deer counts
Forest	1.241	0.224	5.531	3.18e-08	***Strong positive effect:*** more forest → higher deer counts
Residential Development	0.586	0.292	2.006	0.045	*Slight positive effect:* more residential dev. → higher deer counts

Table 5. *Results from the best fit negative binomial model. This model included the amount of agriculture, forest, and residential development within the survey unit. All three covariates had positive effects on the count estimates of deer within a survey unit.*

Table 6. *The results from using the best-fit negative binomial model to predict deer abundance across the entire state. The total estimated abundance and average density per km² are given for each scenario: estimated values assumed correct, minimum estimated value given uncertainty, and maximum estimated value given uncertainty.*

Scenario	Estimated Abundance	95% Confidence Intervals	Mean Density (Deer/km²)	Mean Density (Deer/mile²)
Mean	15,944	14,225 - 17,882	6.14	15.91
Minimum	4,810	3,904 - 5,933	1.85	4.80
Maximum	128,298	125,877 - 130,803	49.42	127.99

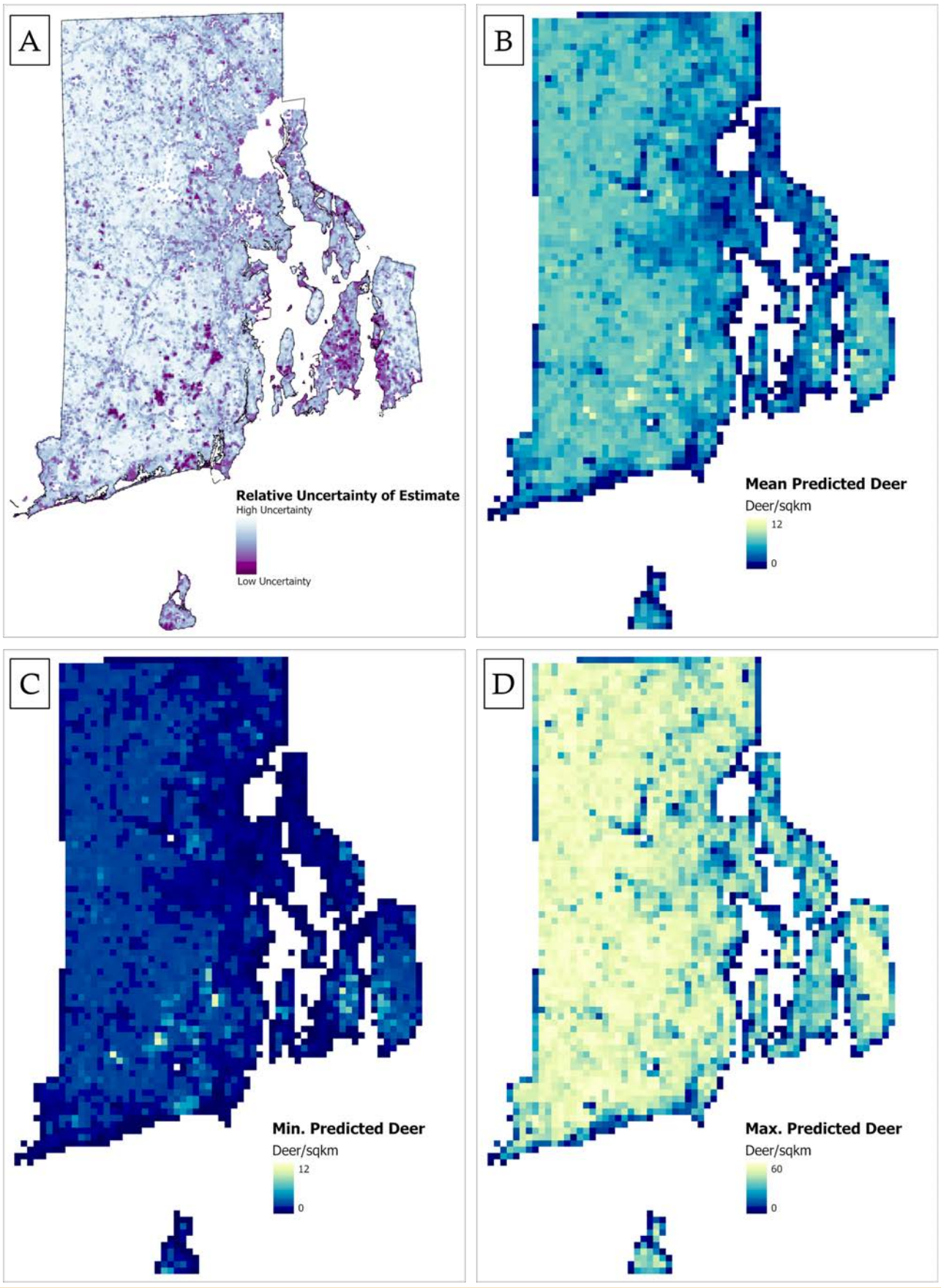

Figure 9. *Spatial predictions of deer/km² under three predictive modeling scenarios: (B) mean, (C) minimum, and (D) maximum deer estimates. We used the difference between the maximum and minimum predictions to show which areas in the state have the highest uncertainty (A), and thus lowest confidence in estimates, to add context to the predicitve abundance estimations.*

Survey Results

Project/ Data Year		Predicted Deer Abundance	95% C.I.	Mean Density (Deer/km²)
Camera Survey	Summer '19	28,708	28,476 - 28,937	11.4
Camera Survey	**Winter '20**	**15,526**	**15,411 - 15,642**	**6.1**
Camera Survey	Summer '20	21,751	21,614 - 21,889	8.6
Camera Survey	**Winter '21**	**22,489**	**22,402 - 22,576**	**8.9**
Camera Survey	Summer '21	23,689	23,594 - 23,784	9.4
Population Reconstruction (Bellier et. al 2024)	Harvest data '12 - '21	21,200	20,502 - 21,439	8.2
Camera Survey	**Winter '22**	**19,408**	**19,332 - 19,485**	**7.7**
Camera Survey	Summer '22	19,579	19,489 - 19,688	7.7
Camera Survey	**Winter '23**	**18,686**	**18,579 - 18,792**	**7.4**
Aerial Survey	**Winter '25**	**15,944**	**14,225 - 17,882**	**6.14**

Table 7. *Abundance estimates from previous analyses: a statistical population reconstruction from harvest data, and abundance estimates from trail camera surveys. (winter season abnudance estimates are highlighted). The mean estimated abundance from the current aerial survey is 15,944 (14,225 - 17,882) with a mean density of 6.14 deer/km².*

Predicted Abundance Results By Survey Area

The predicted density (deer/km²) was overall consistent throughout the survey areas (**Table 8**). The predicted density was highest in the Tiverton/Little Compton survery area, however the overall uncertainty in this survey area was also high (**Figure 9**). The predicted deer density was lowest in the East Bay survey area, however the overall uncertainty in this area was low, meaning we had more confidence in the estimates. Across the entire state, the mean predicted deer densities in 1km² sized cells ranged from 0 to 11.5 deer/km² (0 - 29 deer/mile²) (**Figure 10**).

Table 8. *Predicted abundance and density estimates for each survey area. Wider ranges between the minimum and maximum values indicate higher uncertainty in the predicted values and density estimates. The Tiverton/Little Compton survey area had the highest predicted density, while East Bay had the lowest predicted density. Aquidneck had the lowest overall uncertainty (higher confidence), while Prudence Island had the highest overall uncertainty (lower confidence).*

	Predicted Abundance			Predicted Mean Density	
	Mean estimate	*Min. estimate*	*Max. estimate*	*Deer/km² (min - max)*	*Deer/mile² (min - max)*
Rhode Island	**15,944**	**4,810**	**128,298**	**6 (2 - 49)**	**16 (5 - 128)**
Mainland	13,851	4,036	111,603	6 (2 - 50)	16 (5 - 131)
Block Island	120	45	959	5 (2 - 40)	13 (5 - 103)
Prudence Island	82	20	680	6 (1 - 46)	14 (4 - 119)
Jamestown	139	52	1,115	6 (2 - 45)	14 (5 - 116)
Aquidneck	441	194	3,468	5 (2 - 39)	13 (6 - 100)
East Bay	459	142	4,299	5 (1 - 42)	12 (4 - 108)
Tiverton/ Little Compton	852	320	6,172	7 (2 - 47)	17 (6 - 122)

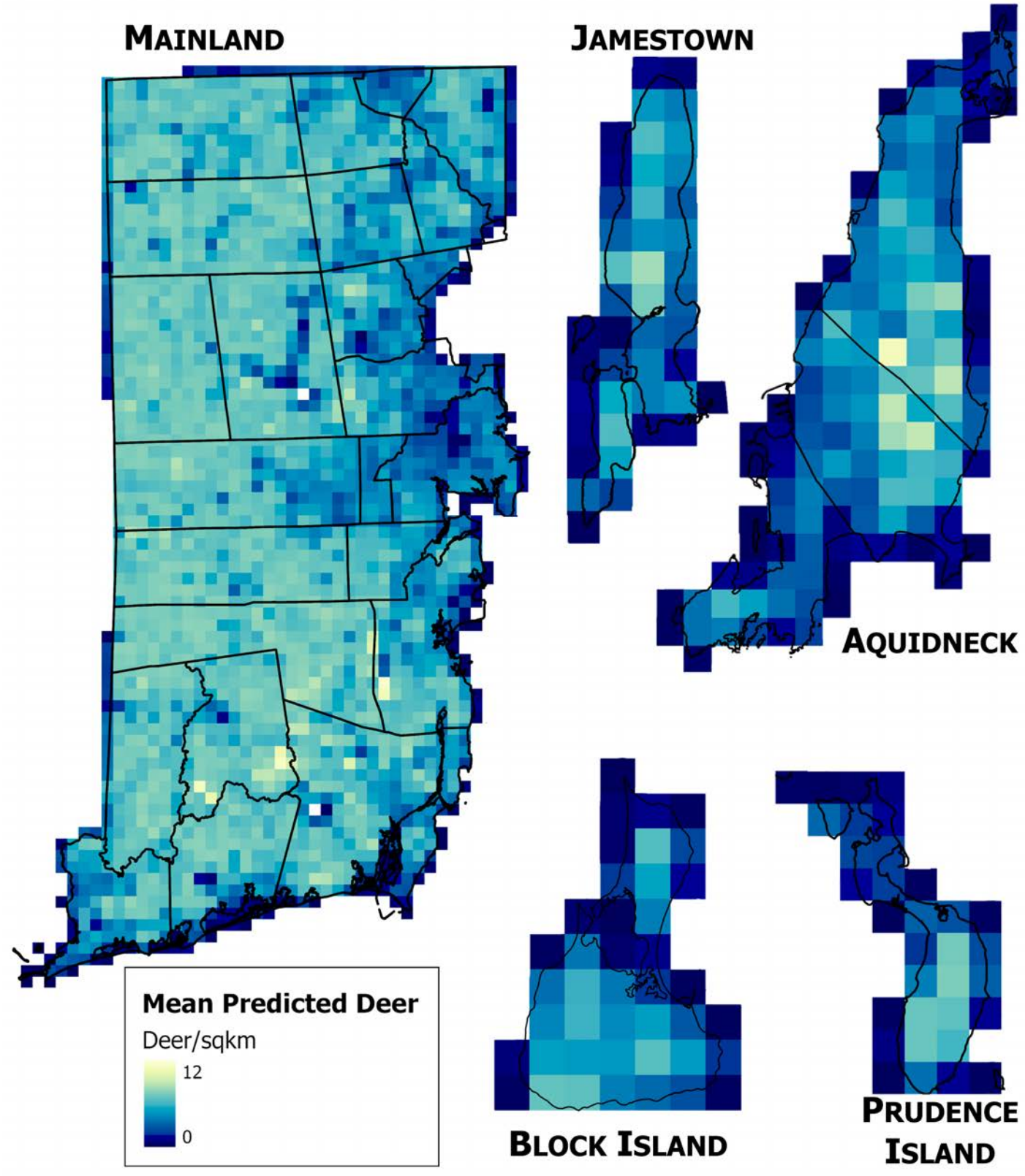

Figure 10. *Maps of mean predicted deer per km² for each survey area. Map cells are 1km², and lighter colors indicate higher predicted deer densities, while darker colors indicate lower predicted deer densities.*

Survey Results

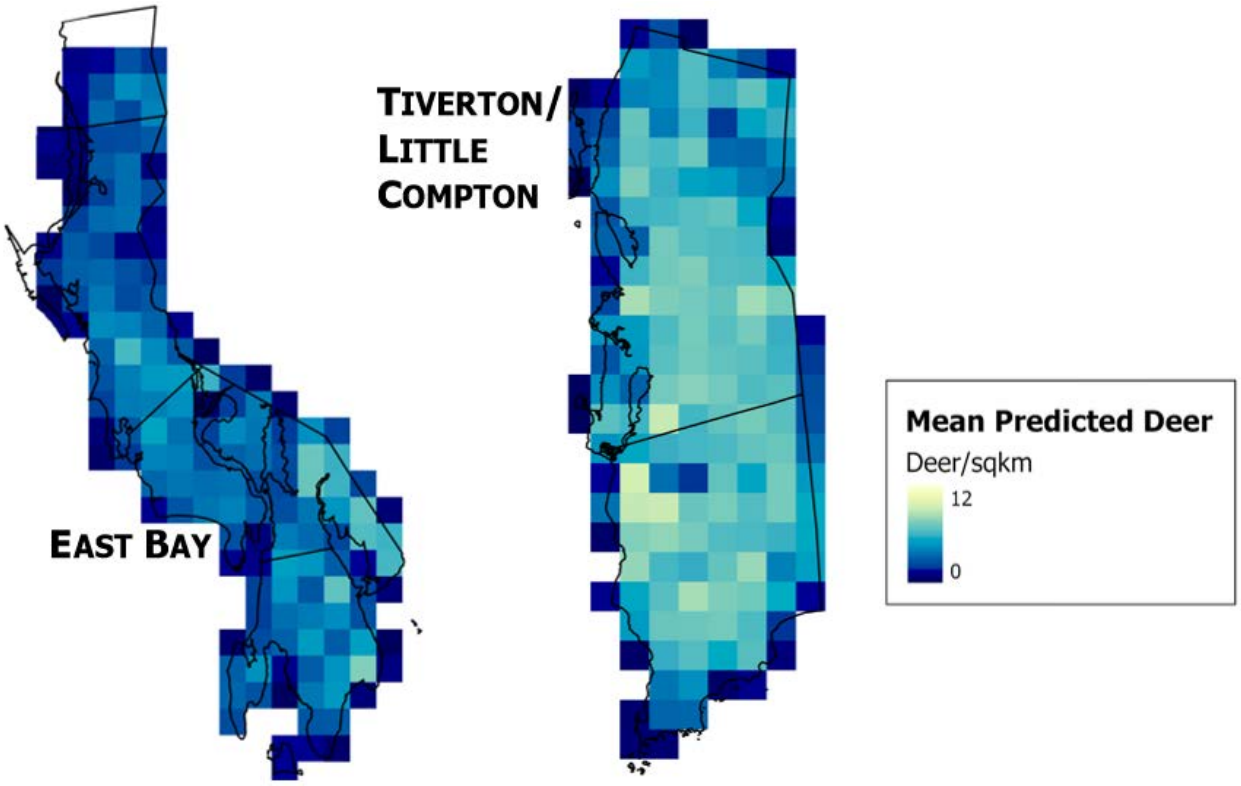

Figure 10 (cont'd). *Maps of mean predicted deer per km² for each survey area. Map cells are 1km², and lighter colors indicate higher predicted deer densities, while darker colors indicate lower predicted deer densities.*

Limitations & Recommendations

The majority of the uncertainty in the estimates generated from this survey can be attributed to the equipment used to collect the imagery. The FLIR Vue Pro R infrared camera is designed for small, unmanned aircraft systems (sUAS), or drones. Standard regulations indicate that drones are usually operated below 400 ft (121 m), while the average altitude flown during these surveys was 266 m. This discrepancy in operating altitude greatly affected the quality of the imagery and ultimately our ability to accurately detect deer from the images (**Figure 11**).

Additionally, there were limitations on the customization of the camera itself, primarily that we could not standardize the scale at which temperatures were recorded on the images. For each image collected (1 per second of flight), the light-to-dark temperature scale of the image was self-adjusted based on the temperatures in that particular image. This prevented us from using any automation to process the images or verify our estimates, as deer could appear lighter or darker in subsequent images, depending on the surrounding environment.

Figure 11. *Increased flight altitude negatively affected the ability to confidently detect deer in the imagery. The image on the left was captured at 189m AGL and was estimated to contain 4 deer with high confidence. The image on the right was captured at 350m AGL and also estimated to contain 4 deer, but with low confidence.*

Limitations & Recommendations

While the pilot completed all flights prior to the cut-off date of April 1, 2024, mild winter conditions meant that by mid-March, conditions had already become unfavorable for optimizing infrared image quality. The early warming conditions meant that vegetation began leafing out, and ground and surface water began flowing, both of which added to significant thermal clutter in the imagery. Additionally, four of the eight surveys had recorded daytime high temperatures above 50°F, and only two of the eight surveys had recorded temperatures during flight below freezing (**Table 2**). These warm daytime temperatures allow vegetation, rocks, and water to absorb and retain heat, which leads to thermal cluttering of the imagery (**Figure 12**). Conducting the surveys during warmer temperatures prevented deer, or any warm-bodied animals, from standing out against the warm backgrounds, thus reducing detection and confidence in estimations. Overall, confidence in estimates was fairly low, and there were limited instances where deer were easily identifiable.

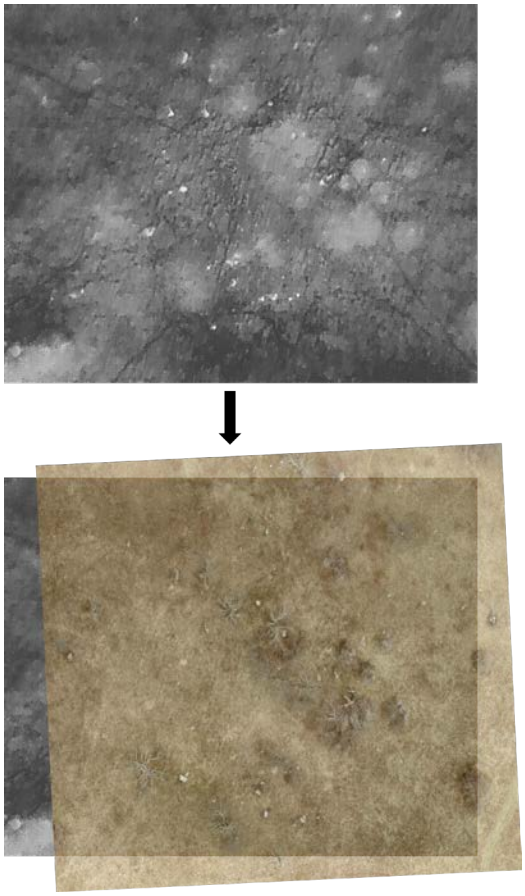

Figure 12. *Warm daytime temperatures allow rocks to collect and retain heat. When processing images, these bright spots can be confused with deer, but comparison with satellite imagery confirms they are rocks.*

Lastly, errors in georeferencing as a result of missing or incorrect metadata prevented us from using a more robust modeling framework for this analysis. Methods that account for detection probability include distance sampling, double observer, and repeat surveys. While we initially intended to follow a distance sampling framework, the quality of the imagery and inconsistencies in georeferencing precluded this from being an appropriate option. As a result, our models do not account for variability in detection probabilities and the estimations provided represent a relative population abundance estimate rather than a true population abundance.

Recommendations for Future Population Studies

Given the limitations of this survey, we do not recommend repeating population surveys using this method in the future. If aerial surveys are required to cover large spatial areas, a more appropriate thermal imaging system should be used that can provide finer-scale imagery from high altitudes. The existing camera system is appropriate for drones/sUAS, which can be flown at lower altitudes than fixed-wing or helicopters, but have stricter flight-area limitations. However, with careful planning of both flight and weather conditions, as well as using stratified sampling across a smaller area, this method may be appropriate for future surveys.

Lastly, given similarities in abundance estimates between previous trail camera surveys and the population reconstruction analysis, as well as the marginal alignment between those estimates and the current estimate from this aerial survey, we recommend continuing trail camera surveys as a potential method for estimating spatial abundance and monitoring population changes. In addition to this method being relatively low-cost/low-effort when compared with the current aerial survey, the data collected from camera studies can easily be paired with other survey methods (aerial surveys, harvest data) to increase accuracy in population estimations.